Tuning the Morphology of Nanostructured Peptide Films by Introduction of a Secondary Structure Conformational Constraint: a Case-Study of Hierarchical Self-Assembly

Marta De Zotti,[a] Beatrice Muzzi,[b] Emanuela Gatto,[b] Benedetta Di Napoli,[b] Claudia Mazzuca,[b] Antonio Palleschi,[b] Ernesto Placidi,[c] Fernando Formaggio,[d] Claudio Toniolo[d] and Mariano Venanzi*[b]

[a] *Department of Chemistry, University of Padova, Via Marzolo 1, 35131 Padova, Italy*

[b] *Department of Chemical Sciences and Technologies, University of Rome 'Tor Vergata', Via della Ricerca Scientifica 1, 00133 Rome, Italy. E-mail: venanzi@uniroma2.it*

[c] *ISM Unit, CNR, Department of Physics, University of Rome 'Tor Vergata', Via della Ricerca Scientifica 1, 00133 Rome (Italy)*

[d] *ICB Unit, CNR, Department of Chemistry, University of Padova, 35131 Padova, Italy*

Abstract

Peptide self-assembly is ubiquitous in nature. It governs the organization of proteins, controlling their folding kinetics and preserving their structure stability and bioactivity. In this connection, model oligopeptides may give important insights on the molecular mechanisms and elementary forces driving the formation of supramolecular structures. In this contribution we show that a single residue substitution, *i.e.* Aib (α-aminoisobutyric acid) in place of Ala at position 4 of an -(L-Ala)$_5$- homo-oligomer, strongly alters the aggregation process. In particular, this process is initiated by the formation of small peptide clusters that promote aggregation at the nanometer scale and, through a hierarchical self-assembly, lead to mesoscopic structures of micrometric dimensions. Furthermore, we show that the use of the well-established Langmuir-Blodgett technique represent an effective strategy for coating extended areas of inorganic substrates by densely-packed peptide layers, thus paving the way for application of peptide films as templates for biomineralization, biocompatible coating of surfaces, and scaffolds for tissue engineering.

1. INTRODUCTION

Formation of peptide nano- and mesoscopic structures of different morphology (globules, fibrils, nanotubes) is currently under intense investigation for its relevance in biomedicine (development of peptide-based materials for tissue engineering, drug-delivery, antimicrobial coating, *etc*.), and in bio-inspired nanotechnology (hybrid materials for optoelectronics, nanocatalysis, biosensing, *etc*.).[1-6]

Peptide self-assembly depends primarily on the structural and dynamical properties of the peptide building blocks, dictated by their amino acid composition and sequence. Electrostatic, van der Waals, and H-bonding interactions, as well as solvation effects, determine the secondary structure attained by the peptide molecules, and, hence, through hierarchical self-assembly (HSA), their organization into nano- and mesoscopic architectures.[7] Environmental conditions (ionic forces, local dielectric constant, pH) and systemic effects (phase segregation) also play an important role.

HSA, *i.e.* the propagation of the structural properties of the peptide building blocks to the mesoscale, has been highlighted in a series of seminal contributions.[8-11] A distinctive feature of HSA is represented by the role of aromatic moieties, which, by specific stacking interactions, rule the ordered arrangement of the molecular units giving rise to superstructures of a given morphology.[12]

Depending on the amino acid sequence and length of the main chain, a polypeptide can attain several ordered conformations, the most common being the canonical α-helix and β-sheet. Other helical structures (3_{10}-, 2.0_5- helices) are also possible, favored by the presence of particular residues or specific peptide motifs.[13]

In this connection, we recently described the unique conformational properties of the α-aminoisobutyric acid, *i.e.* a $C^{\alpha,\alpha}$-dimethylated α-amino acid denoted as Aib or U in the three- or single-letter code, respectively.[14] By use of molecular dynamics simulations it was shown that -$(Aib)_n$-homo-oligopeptides predominantly adopt a 3_{10}-helix structure for the shorter components of the series ($n \leq 8$), evolving to a more stable α-helix for the longer terms.[15] The Aib β-sheet breaker

properties were also recognized, encouraging studies related to the possible utilization of Aib-containing peptides as pro-drugs for neurodegenerative diseases.[16-18]

We recently proved that a single Aib substitution at position 4 of an -(L-Ala)$_n$-homo-pentapeptide strongly altered its conformational landscape and the morphology of the aggregates formed in aqueous solutions.[19] A 2-pyrenyl (Py) group, functionalizing both peptides at their N-terminus, was added to the peptide chain to investigate the role of an aromatic moiety in promoting peptide aggregation and to serve as an intrinsic fluorescent probe. We were able to show that aggregation in methanol/water solutions was mainly driven by the hydrophobic effect, but that the morphology of the mesoscopic peptide aggregates strongly depended on the secondary structure attained by the peptide building blocks. In particular, while the -(L-Ala)$_5$- homo-pentapeptide gave rise to amyloid-like fibrillar structures of nanometric thickness and micrometric length, the Aib-substituted peptide formed almost exclusively micrometric globules.

In this contribution, we used the Langmuir-Blodgett (LB) technique on the same pentapeptide and its Aib-analog previously investigated in methanol/water solutions, to analyze how the different conformational features of the two compounds would affect the aggregation process at the air/water (a/w) interface and the final morphology of the mesoscopic aggregates.

Ultrathin films of organic molecules can be easily obtained by well-established LB methodologies, by which a highly diluted solution of amphiphilic molecules in a volatile solvent is spread on the water sub-phase.[20] Once the solvent is evaporated, the surface pressure is increased by closure of the mobile barriers of the trough, forcing the molecules to interact. During the compression of the mobile barriers, the organic layer at the a/w interface undergoes several phase transitions, until a 2D-ordered film is formed. Eventually, at high surface pressures, the system collapses to a so-called solid phase (S), characterized by formation of 3D aggregates.[21] Onset of the film at the a/w surface is controlled by monitoring the surface pressure (π) as a function of the mean area occupied *per* molecule (Mma). The nature and extent of the intermolecular interactions determine the LB film morphology at intermediate π values and the structure of the supramolecular aggregates at high

surface pressures. In addition, the π/Mma isotherms allow one to establish the most suitable conditions for depositing the organic layer on a solid substrate as a dense and homogeneous film, paving the way for applications.

It should be noted that peptide aggregation at the a/w interface has recently been studied for mimicking the toxic interaction between amyloid peptides and lipid membranes.[22] In particular, IR absorption spectroscopy measurements of LB films revealed that amyloid peptides at the a/w interface can adopt a β-sheet conformation, *i.e.* the precursor of peptide fibrillation.[23] In the same connection, it has been also demonstrated that amphiphilic peptides, *i.e.* peptides with alternating apolar and polar residues producing amyloid-like fibers in solution, can form β-sheet monolayers at the a/w interface.[24,25]

Therefore, investigation of peptide aggregation at the a/w interface may offer significant information on the activity of amyloids at the lipid surface. On the other hand, from the point of view of hybrid materials nanotechnology, LB methods can be applied to control the morphology of peptide films coating extended areas of inorganic substrates. These two aspects are the principal source of inspiration for this work.

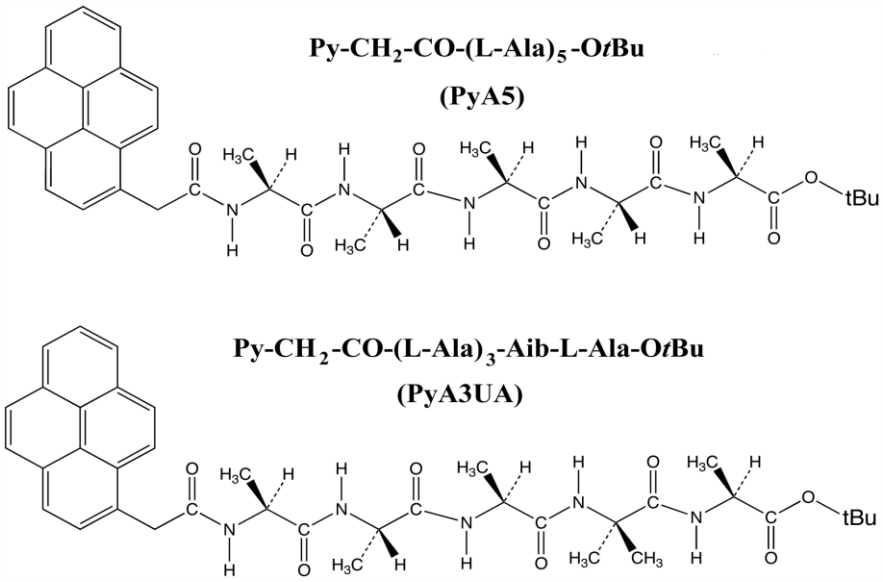

Schematic 1. Molecular formulas and acronyms of the two pentapeptide analogs investigated in this work.

2. EXPERIMENTAL SECTION

MATERIALS

The synthesis and characterization of the two pentapeptide analogs investigated, denoted in the following as **PyA5** and **PyA3UA**, have already been published elsewhere.[19] Molecular formulas and acronyms are reported in Schematic 1 for clarity.

SPECTROSCOPY

UV-Vis absorption measurements were carried out on a Varian Cary 100 (Varian Inc., Palo Alto, CA) spectrophotometer. Steady-state fluorescence experiments were performed on a SPEX Fluoromax-4 spectrofluorimeter (Jobin Yvon-SPEX, Edison, NJ) operating in the single photon counting (SPC) mode. Fluorescence measurements on peptide LB films were carried out on a quartz support fixed on a rotating holder placed at 45 degrees with respect to the excitation beam in order to minimize diffuse light contamination.

Fourier-transform infrared (FTIR) absorption spectra of peptide films obtained by LB deposition were measured on a Thermo Fisher iS50 spectrophotometer (Thermo Fisher Scientific Co., Madison, WI) in the attenuated total reflection (ATR) mode using a ZnSe cell. Each spectrum was recorded mediating over 128 scans with a resolution of 2 cm^{-1}. Deconvolution of the FTIR-ATR spectra in the amide I and amide II (1800-1500 cm^{-1}) regions was carried out by using the OMNIC software. Optimizations of peak position and full width at half height (FWHH) of the IR absorption bands were performed by the Fletcher-Powell-McCormick algorithm.[26]

LANGMUIR-BLODGETT DEPOSITION

0.1 mg/ml chloroform solutions of the peptides investigated were spread onto a Milli-Q water sub-phase at 20°C. After evaporating the solvent for 20 min, the monolayer formed at the a/w interface was compressed and the surface pressure *vs.* the mean molecular area (π/Mma) isotherm was recorded at a constant compression rate of 10 mm/min. The molecular film was transferred by

the vertical lifting method onto a 10x45 mm^2 quartz substrate, previously treated with a piranha solution for 15 min, washed with Milli-Q water and ethanol and subsequently dried with a gentle flux of argon. Peptide films were transferred by lowering and raising the substrate in and out from the aqueous sub-phase. Measurements of π/Mma isotherms and deposition of multilayer films were carried out using a computer-controlled KSV (KSV MiniMicro, Helsinki, Finland) LB apparatus.

MICROSCOPY EXPERIMENTS

Atomic force microscopy (AFM) measurements were performed in air by use of a Veeco Multiprobe IIIa (Veeco, Santa Barbara, CA) instrument. **PyA5** and **PyA3UA** monolayers were deposited by the LB method on mica, previously washed with Milli-Q water and ethanol, and then dried with a flux of argon at a fixed surface pressure. Experiments were carried out at room temperature (20° C) in the tapping mode using Si tips with a spring constant of about 40 N/m and a typical curvature radius on the tip of 7 nm.

MOLECULAR DYNAMICS

Molecular dynamics (MD) simulations for **PyA5** and **PyA3UA** monolayers at the a/w interface were performed using the software GROMACS 4.6.7[27] and the GROMOS53a6 force field.[28] To this aim, two symmetrical monolayers, each formed by 16 peptide molecules, were created in a 9x9x27 nm^3 simulation box. The two peptide monolayers were separated by a 3-nm thick slab comprising 8715 water molecules (SPC model).[29] A 27 nm long (z) dimension was taken into account to eliminate interactions between the periodic images of the system. The peptides, initially attaining an extended conformation, were positioned in the simulation box in a perpendicular arrangement with respect to the water surface. Energy minimization was therefore carried out by a two-step procedure, minimizing the energy of the solvent molecules at first and then the solute energy, before starting with the MD simulations. The solvent was equilibrated using a 150 ps MD at 50 K, while the 16 peptide molecules were restrained. The system was gradually heated to 300 K through a 1 ns MD simulation before the 50 ns production run. The equilibration step, the heating step, and the production simulation were carried out using a 2 fs time step, the PME algorithm[30] for

electrostatics with a double cut-off at 1.4 nm for van der Waals interactions, and the Berendsen algorithm[31] for both temperature (coupling constant: τ_T = 0.2 ps) and pressure (τ_P = 1 ps, *semi*-isotropic conditions) couplings.

The topology needed for the 2-methylpyrenyl group was obtained from the Automated Topology Builder and Repository,[32] while the topology for Aib was developed using the Ala parameters as reference.[15] Both peptides were capped at the C- and N-termini with a *tert*-butoxyl (O*t*Bu) and a 2-carboxymethylpyrenyl group, respectively.

3. RESULTS

3.1 PEPTIDE FILM FORMATION AT THE AIR/WATER INTERFACE

The aggregation process at the a/w interface of the two pentapeptides was monitored by recording the π *vs.* Mma LB isotherms (Figure 1). It can be seen that, while those obtained by adding increasing volumes of **PyA5** chloroform solutions on the top of the water sub-phase are strictly overlapping, in the case of **PyA3UA** a remarkable dependence of the LB isotherms on the peptide surface concentration can be observed. In particular, the critical Mma value, at which the liquid expanded (LE) to liquid condensed (LC) phase transition takes place, occurs at about 30 Å^2/molecule for **PyA5**, almost independently on the added volume of the peptide solution. In the case of **PyA3UA**, this value markedly decreases from approximately 110 Å^2/molecule for 70 µl and 90 µl added volumes, to 90 Å^2/molecule (130 µl added) and 70 Å^2/molecule (160 µl added). For comparison, it should be considered that the area covered by the two peptides in their extended conformation is about 195 Å^2 when they are placed flat on the water phase, and about 72 Å^2 when arranged vertically to the surface.

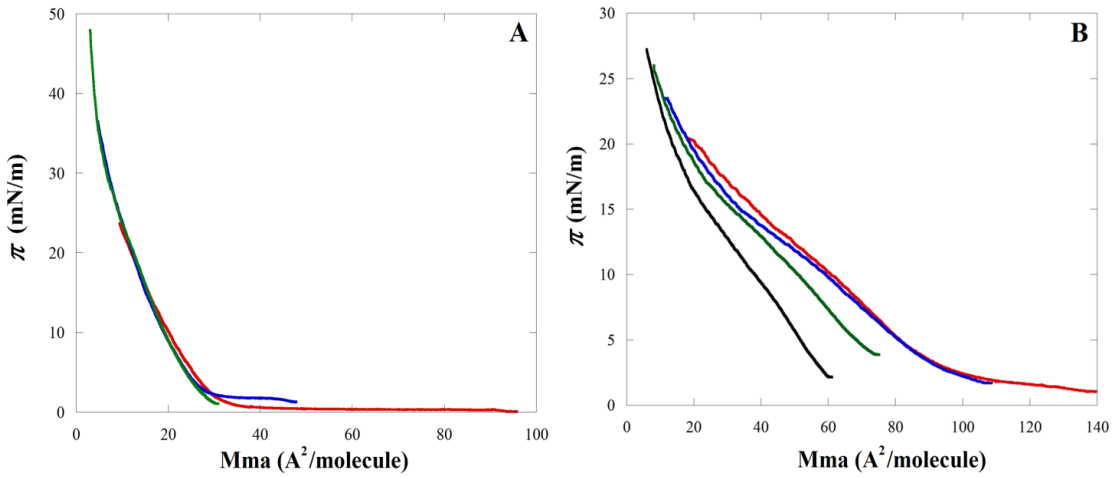

Figure 1. Surface pressure (π) *vs.* Mma isotherms of different volumes of 0.1 mg/ml **PyA5** (A: red = 100 µl; blue = 200 µl; green = 210 µl) and **PyA3UA** (B: red = 70 µl; blue = 90 µl; green = 130 µl; black = 160 µl) chloroform solutions spread at the a/w interface of a LB trough.

It has been suggested that horizontally oriented helices partially changed their orientation to vertically oriented upon compression in the plateau region of the isotherm.[33] Alternatively, it can be hypothesized that the floating film at first forms a multilayer structure or small peptide clusters, evolving to mesoscopic aggregates upon further compression.[34]

It should be noted that for all the added volumes, the onset of the LE→LC phase transition occurs at much lower Mma values for **PyA5** than for **PyA3UA**. These results strongly suggest that **PyA5** can be easily packed as a dense film at the a/w interface, giving rise to the same compact structure independently of the peptide concentration on the water surface.

In the case of **PyA5**, a fast rising of the surface pressure with lowering of Mma is observed, until at π higher than 35 mN/m a steep rise of the LB isotherm takes place, signaling the 3D collapse of the film (solid phase, S) at π =65 mN/m. At this surface pressure, the Mma value is less than 10 Å^2/molecule, indicating the formation of 3D peptide aggregates. On the basis of these results, we decided to deposit the **PyA5** film on the solid substrate at π = 30 mN/m, *i.e.* at the end of the LE→LC phase transition.

In the case of **PyA3UA**, in the region of the LB isotherm comprised between 80 and 40 Å^2/molecule, and depending on peptide concentration, a definitely slower increase of the surface pressure is seen, with a characteristic inflection of the curve, suggesting that, in a certain surface pressure region, LE and LC phase domains coexist. At Mma values lower than 30 Å^2/molecule, the surface pressure increases with a stiffer rise, without however exceeding 30 mN/m, where the collapse of the film (LC→S transition occurs. Under these conditions, the **PyA3UA** films are deposited on the solid substrates at π = 15 mN/m.

Cyclic LB isotherms reveal further important differences in the aggregation properties of the two peptides at the a/w interface. As can be seen from Figure 2, in analogy with the concentration-dependent curves reported in Figure 1, consecutive LB isotherms of **PyA5** are almost overlapping, while those of **PyA3UA** are markedly shifted to lower Mma values at each consecutive compression/expansion cycle.

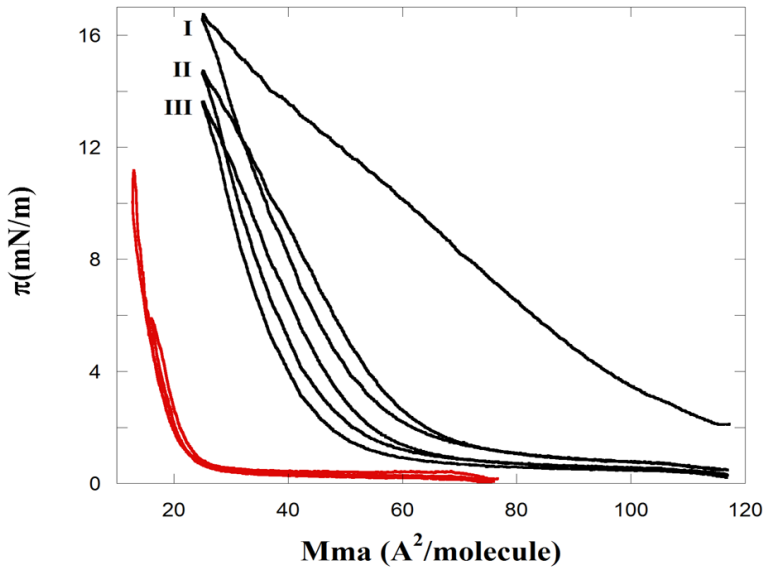

Figure 2. Consecutive compression/expansion cycles (LB isotherms) for **PyA5** (red) and **PyA3UA** (light blue).

These results indicate that **PyA5** aggregation at the a/w interface can be considered a *quasi*-reversible process, following the same aggregation pathway at each compression/expansion cycle, and, most likely, attaining the same compact structure. The remarkable hysteresis observed in the

case of **PyA3UA** is suggestive of irreversible changes caused by compression of the peptide film, probably due to formation of heterogeneous 3D aggregates.[35] Further differences are made evident by considering the variation of the surface compressibility modulus of the two compounds during formation of the peptide films. The surface compressibility factor (K) is defined as

$$K = -A\left(\frac{d\pi}{dA}\right)_T \qquad (1)$$

Basically, the higher the value of K, the tighter is the lateral packing of the molecules. The K *vs.* Mma isotherms of **PyA5** and **PyA3UA** are reported as Supporting Information (Figure S1). Interestingly, while **PyA5** shows polydispersed K values with a peak at approximately Mma = 20 Å^2/molecule, **PyA3UA** exhibits a narrow K *vs.* Mma band, with a peak at definitely larger Mma values (≈80 Å^2/molecule). Furthermore, while in the low Mma region **PyA3UA** features relatively low compressibility factors, **PyA5** shows a steep rise of K, indicating a tight packing of **PyA5** at high surface pressures.

3.2 SPECTROSCOPIC STUDIES OF PEPTIDE FILMS ON QUARTZ

Mono- and multilayer films of **PyA5** and **PyA3UA** were deposited by the LB technique on a hydrophilic quartz substrate for spectroscopic studies at π = 30 and 15 mN/m, respectively.

3.2.1 FLUORESCENCE EXPERIMENTS

Steady-state fluorescence studies were carried out on **PyA5** and **PyA3UA** multilayers immobilized by LB deposition on a quartz substrate (Figure 3). Interestingly, the spectrum of **PyA5** is dominated by the excimer emission, characteristic of an ordered array of stacked pyrene chromophores.[36] Notably, the excimer emission intensity steadily increases as the number of peptide layers increases, suggesting an ordered stratification of the **PyA5** layers on the solid substrate for successive LB emersion/immersion steps.

It should be noted that such excimer emission was found to be definitely less intense in the fluorescence spectrum of **PyA5** in methanol/water solutions under aggregating conditions (see for

comparison Figure 4A in Ref. 19). This finding indicates a very different spatial organization of the pyrene units in the peptide aggregates formed in solution and in the LB film.

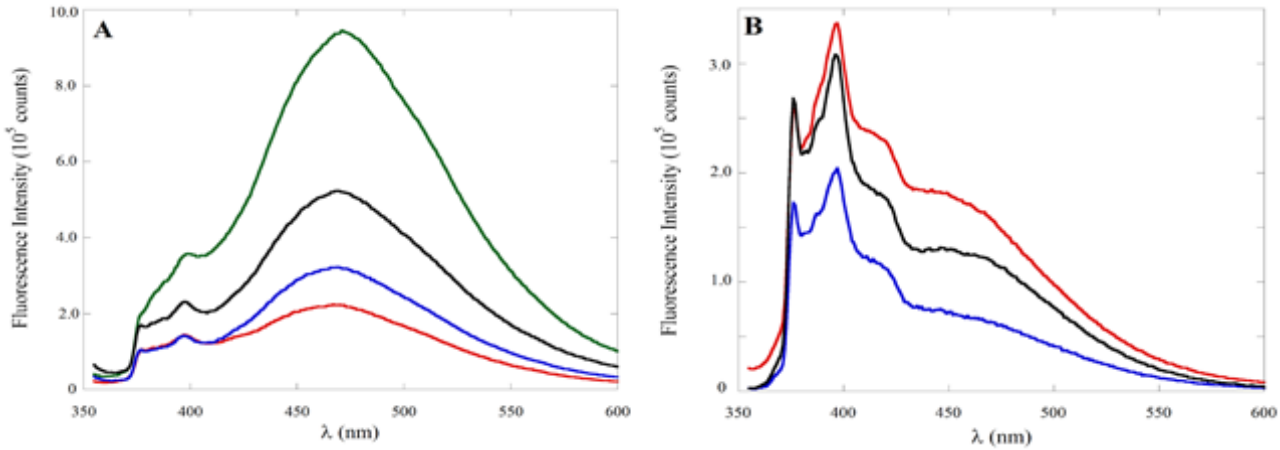

Figure 3. Fluorescence emission spectra of **PyA5** (A; red: 1 layer; blue: 3; black: 7; green: 13) and **PyA3UA** (B; red: 1 layer; blue: 3; black: 7) multilayers on a quartz substrate.

On the contrary, the pyrene emission in **PyA3UA** is characterized by a monomer-like spectrum, with only a minor contribution from the excimer species. In addition, the emission intensity changes randomly for the **PyA3UA** films formed through a different number of LB emersion/immersion steps, pointing to a not homogenous coating of the substrate.

3.2.2 FTIR-ATR ABSORPTION SPECTROSCOPY

FTIR-ATR absorption measurements were carried out on LB films of **PyA5** and **PyA3UA** to obtain information on the secondary structure adopted by the peptide building blocks immobilized in the multilayer coating the quartz/ZnSe substrate. In the case of the -(L-Ala)$_5$- homo-pentapeptide, the FTIR-ATR spectrum (Figure 4A) shows very sharp absorption bands centered at 3300 cm^{-1} (N-H stretching), 1620 cm^{-1} (amide I), and 1530 cm^{-1} (amide II). These spectral regions are close to those already reported for β-sheet forming (L-Ala)$_n$ *n* = 5-7 sequences with different terminals in the solid state.[37,38] The FTIR-ATR absorption bands of the **PyA3UA** LB film (Figure 4B) appear definitely broader than those obtained for the **PyA5** film, indicative of a higher conformational heterogeneity in the former.

The Amide I band is widely used to analyze the peptide conformational properties, as different secondary structures give rise to characteristic absorption bands in this region. Typically, the α-helix absorption band is observed in the 1650-1660 cm^{-1} range, while absorption bands in the 1615-1627 cm^{-1} range are ascribed to intermolecular β-sheets. 3_{10}-helices and turns are generally observed at higher energies, *i.e.* at 1660-1670 and 1680-1690 cm^{-1}, respectively.[39] Deconvolution of the Amide I absorption band shows that for **PyA5**, the component centered at 1626 cm^{-1} largely predominates, the other components observed at 1650 and 1685 cm^{-1} accounting for less than 10% of the Amide I total area (Supporting Information, Figure S2). On the contrary, for **PyA3UA**, several components of comparable intensities, centered at 1627 (β sheet), 1650 (α-helix), 1668 (3_{10}-helix) and 1687 cm^{-1} (β-turn), were detected by deconvolution of the FTIR absorption spectrum in the same region. Besides that, in the amide A region, an absorption band (≈3440 cm^{-1}) typical of free NH groups, *i.e.* NH groups not involved in H-bonding interactions, was also measured, confirming the heterogeneous conformational landscape of the Aib-substituted pentapeptide.[40]

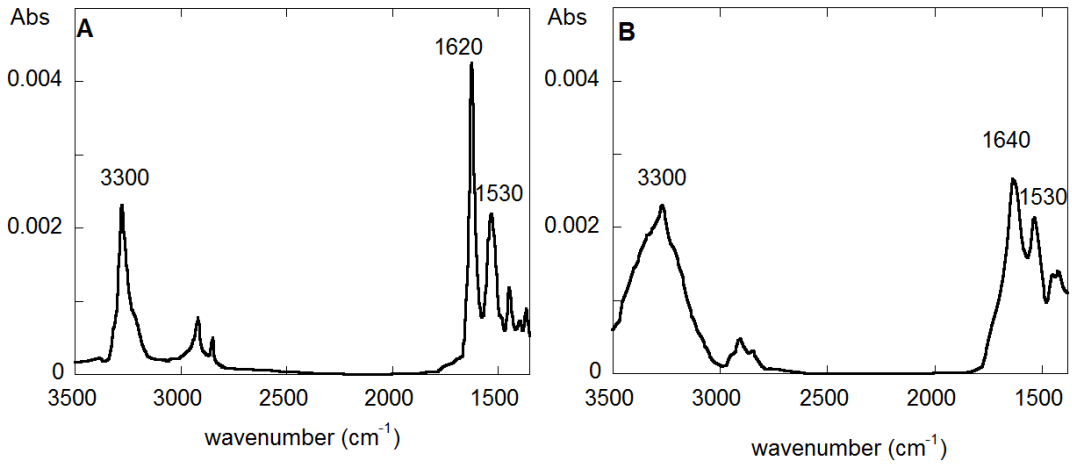

Figure 4. FTIR-ATR spectra of **PyA5** (A) and **PyA3UA** (B) Langmuir-Blodgett films immobilized on a quartz substrate.

Spectroscopic data, therefore, suggest that, while **PyA3UA** adopts multiple conformations, causing some heterogeneity of the LB film morphology, **PyA5** forms well-ordered β-sheet domains under

the surface pressure conditions of LB deposition. These findings are of some interest because β-sheet ladders are well-known to nucleate the growth of fibrils and micrometric filaments, precursor of the formation of the large amyloid plaques responsible for several neurodegenerative diseases.

3.3 AFM IMAGING OF PEPTIDE FILMS

PyA5 and **PyA3UA** LB monolayers were deposited on mica for AFM characterization of the peptide film morphology with nanometric resolution. A gallery of AFM images obtained for a **PyA5** monolayer deposited at π=30 mN/m on mica are reported in Figures 5 and 6. Interestingly, Figure 5A shows the presence of both micrometric globular structures and long peptide fibers of nanometric thickness. Figure 5B, taken in a different region of the same specimen, exhibits a densely-packed array of peptide fibers, the details of which is shown with higher resolution in Figure 5C. AFM height profiles, taken along the long white line section in Figure 5C, and reported in Figure 5D, reveal that the imaged peptide fibers have thicknesses ranging from 10 to 30 nm and micrometric lengths.

The AFM images reported in Figure 5 also show that the packing of the peptide fibers occurs with a remarkable orientation order, as a result of both attractive interactions between the peptide fibers and the compression exerted by the mobile barriers of the LB equipment.

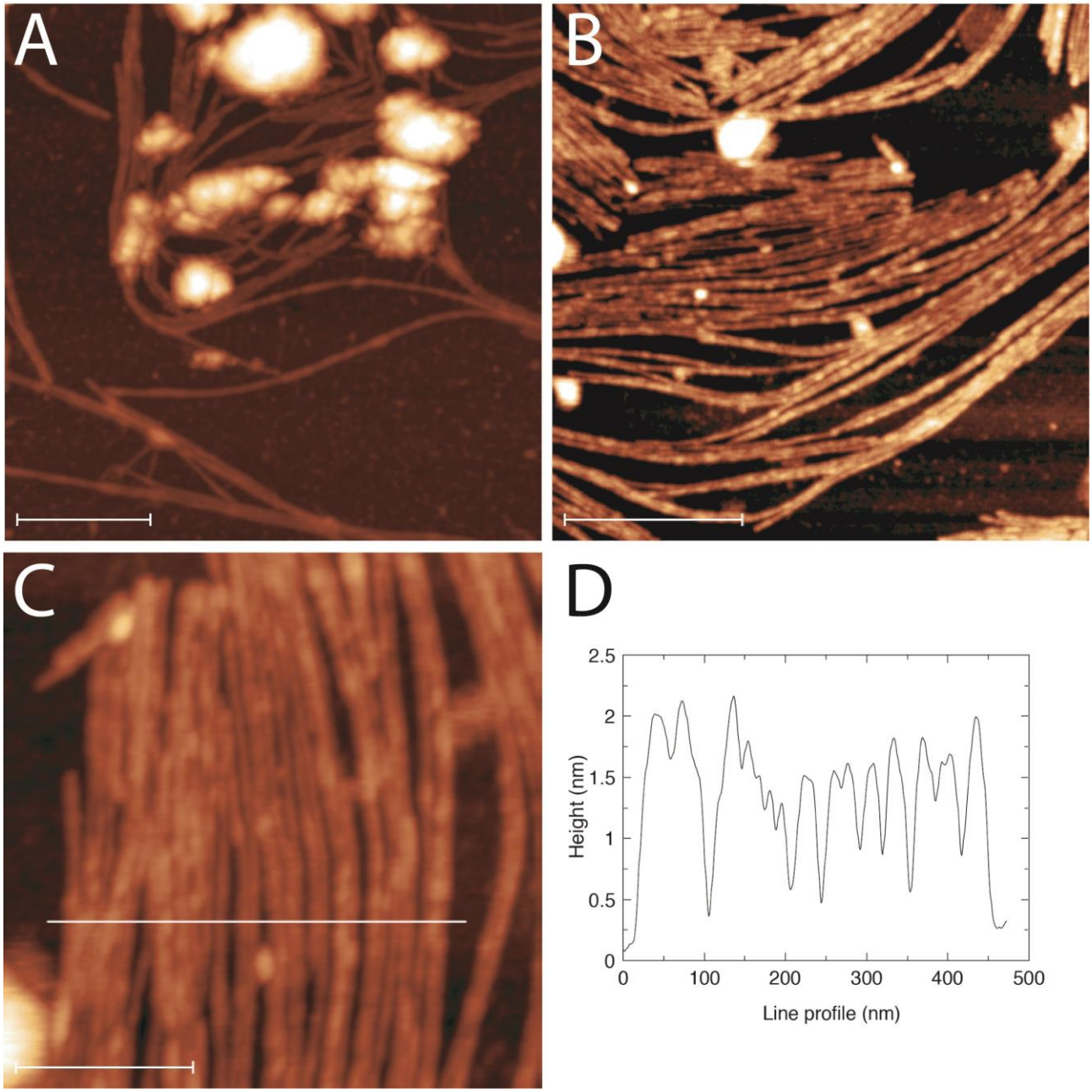

Figure 5. AFM images of a **PyA5** Langmuir-Blodgett film deposited on mica at π=30 mN/m. White bars denote the length scale of the figures A (600 nm), B (300 nm) and C (100 nm). The height profiles shown in Figure D are taken along the long white line crossing the peptide fiber array imaged in Figure C.

Recently, we have shown that **PyA5** in water/methanol solutions forms amyloid-like aggregates because of the combined effect of hydrophobic interactions, the ordered secondary structure of the peptide chains, and the J-type stacking interactions between the Py groups.[19] In that case, AFM imaging of **PyA5** dried on mica after overnight deposition from a methanol/water solution under aggregative conditions only showed *spaghetti*-like structures, *i.e.* intertwined micrometric filaments without apparent ordering (see Figure 8 in Ref. 19).

A very interesting feature, giving some insight into the process of fiber growth and formation, is represented by the AFM images reported in Figure 6, where, like pearls in a necklace, nanometric peptide globules are chained by micrometric filaments, indicative that peptide fibers grow directly from globular structures.

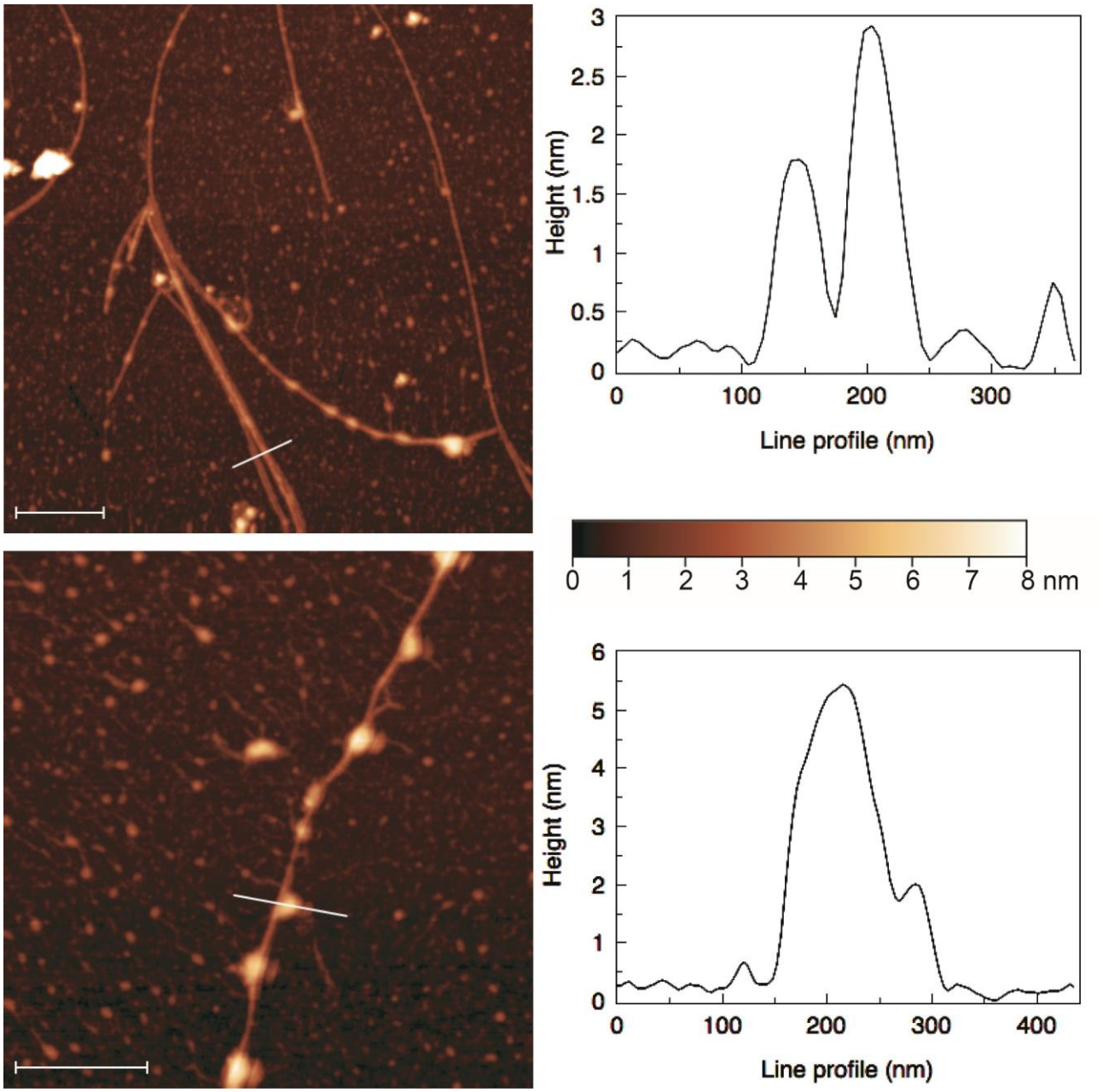

Figure 6. AFM images of a **PyA5** Langmuir-Blodgett film (π=30 mN/m) on a mica substrate. On the right, the height profiles taken along the white lines drawn on the left images are reported. Length scale bars are 800 nm for the top and 500 nm for the bottom images on the left, respectively.

It should be considered that formation of fibers requires the asymmetric growth of peptide aggregates and that the conformational properties of the peptide strongly affect the formation of the small peptide clusters seeding the aggregation process. Interestingly, in a kinetic study of protein aggregation carried out by super-resolution fluorescence techniques, it was found that globular

species, first observed after two hours, continued to be seen after longer times in apparent coexistence with fibers and fiber assemblies, suggesting the continuous growth of fibers upon addition of protein monomers.[41]

In the AFM experiments carried out on **PyA3UA** LB films immobilized on mica, only micrometric globular structures could be imaged, as evident from Figure 7. In particular, neither mature (micrometric) peptide fibrils, or incipient fibrillation of the globular structures observed on the mica surface could be found. The same effect was observed by AFM imaging of **PyA3UA** dried on mica after overnight deposition from methanol/water solutions where only micrometric globular structures were obtained (Figure 9 in Ref. 19).

These findings indicate that the perturbation of the conformation and dynamics of **PyA5** induced by the single Aib *vs* Ala substitution characterizing the **PyA3UA** analog, strongly affects the hierarchical self-assembly process of the peptide building blocks in solution and at the a/w interface.

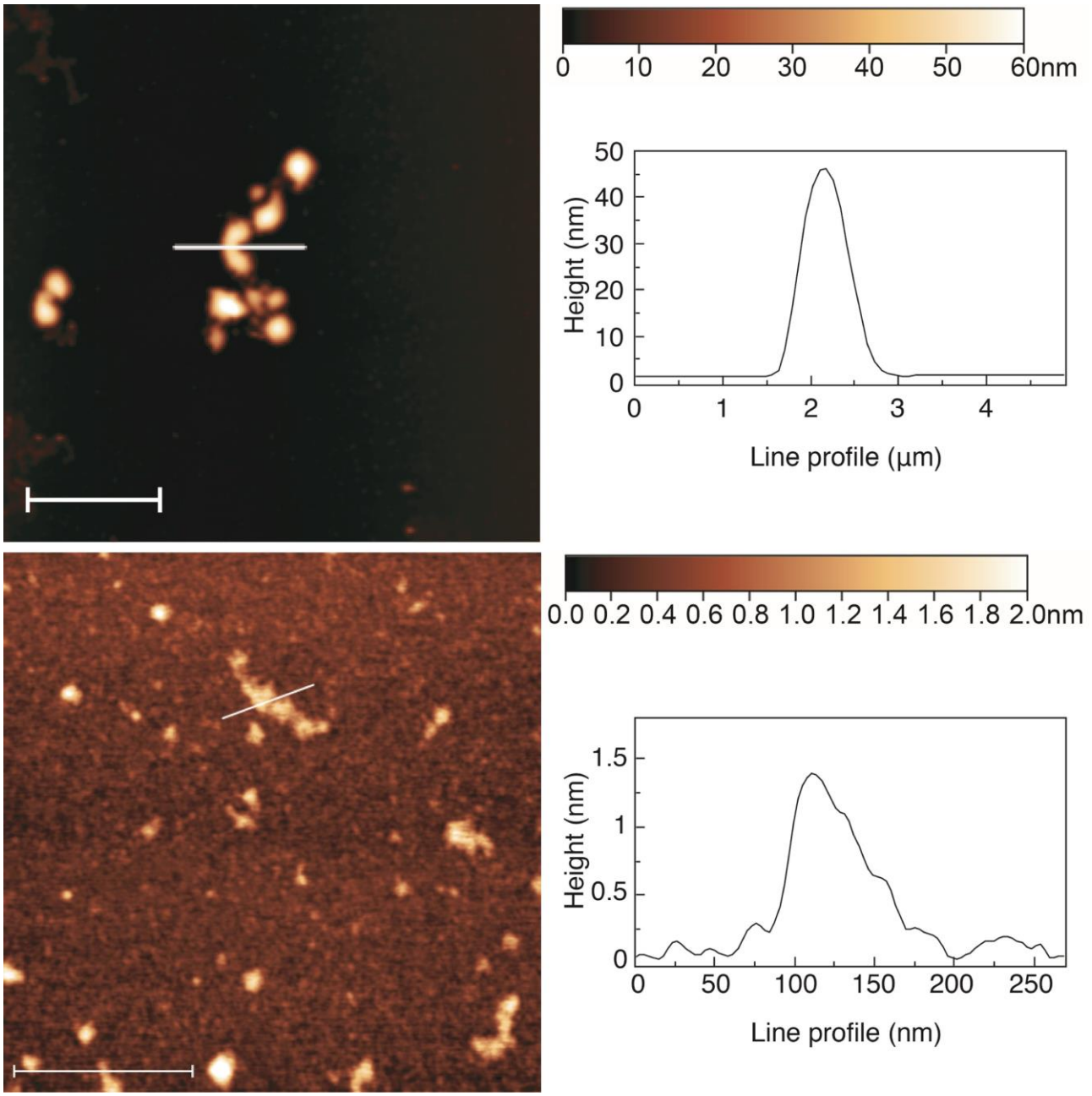

Figure 7. AFM images of a **PyA3UA** Langmuir-Blodgett film on mica. On the right, the height profiles taken along the white lines drawn on the left images are reported. Length scale bars are 5 µm for the top and 500 nm for the bottom images on the left, respectively.

3.4 MOLECULAR DYNAMICS SIMULATIONS

MD calculations were carried out to investigate formation of the small peptide clusters nucleating the aggregation process of the two peptide analogs under study. In Figure 8, the side- (A,D) and

top- (B,E) views of the aggregates formed by 16 molecules of **PyA5** and **Py3AUA** at the a/w interface after a 50 ns MD simulation are reported, respectively. Figures 8C and 8F show the same structures excluding the water molecules for an easier visualization. It can be seen that the 16-molecule **PyA5** cluster attains an ordered disposition, with the Py aromatic groups showing a helical arrangement and the peptide chains almost regularly aligned, mimicking a β-sheet array. On the contrary, the 16 **PyA3UA** chains form a compact structure, with evidence neither for an ordered stacking of the aromatic moieties nor for a regular alignment of the peptide chains. These findings clearly emphasize the effect of the conformational constraint imposed by the Aib residue and its influence on the morphology of the peptide clusters.

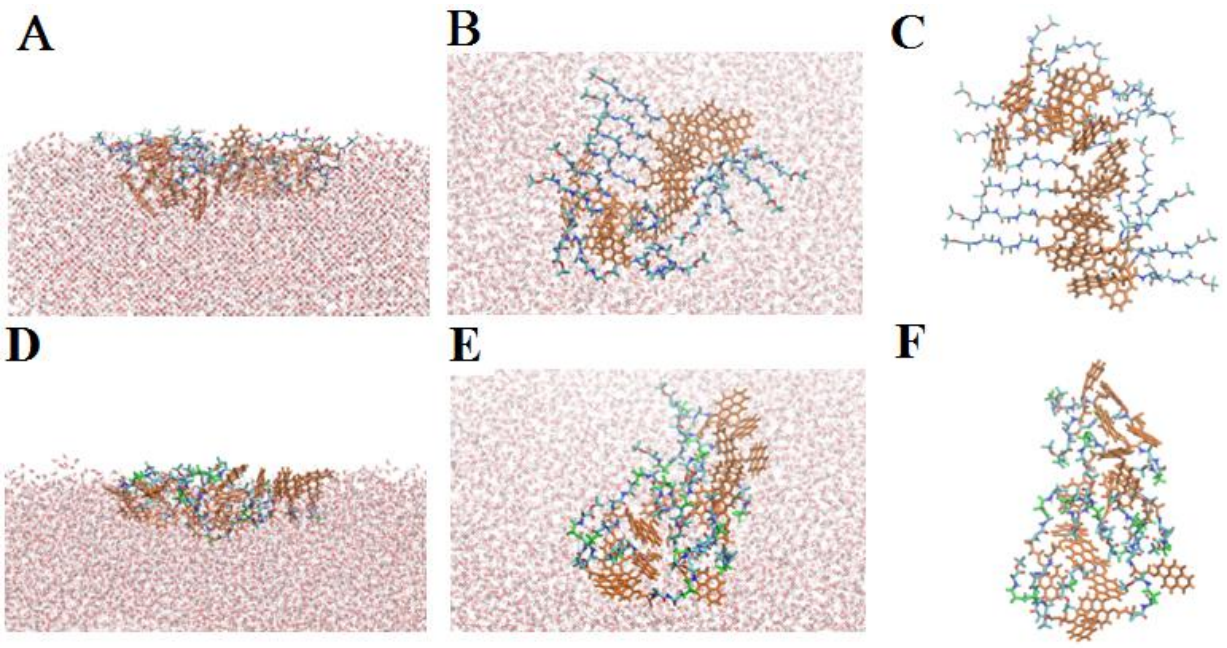

Figure 8. Structures of the aggregates formed by **PyA5** (A-C) and **Py3AUA** (D-F) at the a/w interface after 50 ns. In the MD simulations 16 peptide and 8715 water molecules were considered. A,D: side-view; B,E: top view; C,F: water molecules excluded for clarity. Orange: Py; cyan: Ala; green: Aib.

These considerations are well illustrated by analyzing the radial distribution function *g*(r) of the distances between the centers of mass of adjacent peptide chains (Figure 9A) and between vicinal

Py groups (Figure 9B), obtained by 50 ns MD simulations. While for **PyA5** a regular ladder of Py··Py and peptide chain···peptide chain g(r) peaks can be readily observed, in the case of **PyA3UA** such regularity is rapidly lost with increasing the distance. In particular, in the case of **PyA5** the g(r) peaks of the radial distribution functions of the peptide···peptide interstrand distances occur at multiple values of 4.8 Å, as expected for a β-sheet arrangement of the peptide chains.[42] Significantly, the two g(r) distributions reported in Figure 9 are strongly correlated, indicating that both aromatic and H-bonding interactions concur to stabilize the ordered arrangement of the peptide chains forming the **PyA5** cluster. Furthermore, considering the relative orientation of the interstrand Py groups, it was found that in the case of **PyA5**, the distribution is squeezed toward low θ values (parallel Py··Py orientation), while in the case of **PyA3UA** the orientation distribution is shifted to larger θ values (perpendicular arrangement of vicinal Py··Py groups) (Supporting Information, Figure S3). Clearly, these findings agree with our fluorescence results that show an intense excimer emission for the **PyA5** compound only.

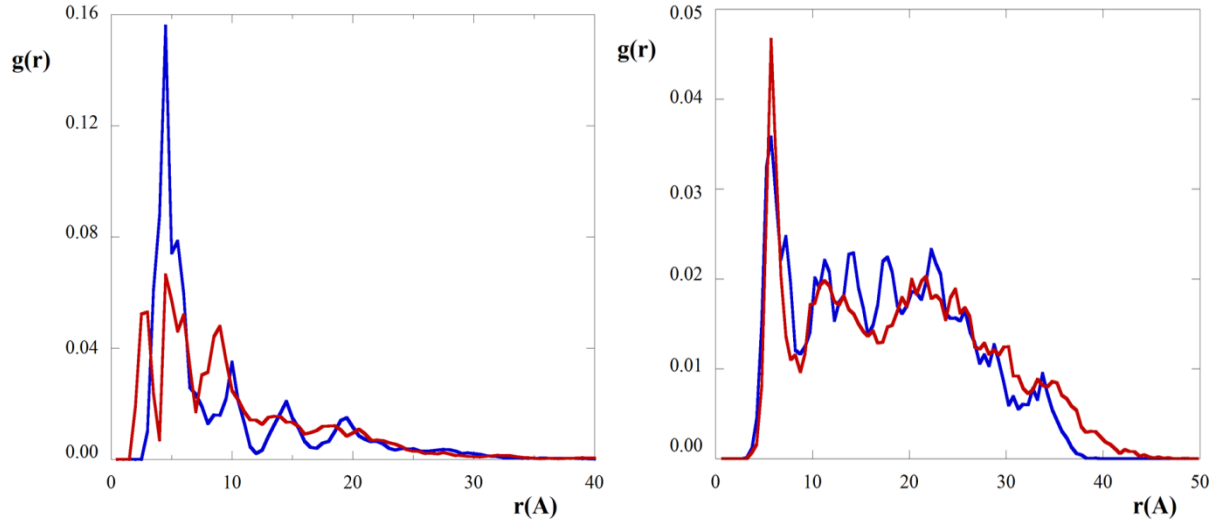

Figure 9. Radial distribution function [g(r)] of the interstrand distances (*r*, Angström) between the centers of mass of adjacent peptide chains (A) and Py groups (B) in the aggregates formed by 16 **PyA5** (blue) and **PyA3UA** (red) molecules at the a/w interface.

4. DISCUSSION

The results reported above demonstrate that, like hydrostatic pressure in solution,[43] the surface pressure can be used for modulating the aggregation process at the a/w interface of self-assembling peptides.

The hysteresis observed in the **PyA3UA** compression/expansion isotherm cycles strongly suggests formation of 3D structures at relatively low surface pressures.22check Such hysteresis was not observed in the case of **PyA5**, indicating that the peptide secondary structure strongly affects the aggregation process, and specifically the LE-LC transition and the collapse to the solid-like phase. This view is reinforced by the AFM imaging results, that revealed definitely different morphologies of the mesoscopic structures formed by the two pentapeptide analogs. The link between the sub-nanometer scale of the secondary structure attained by the single peptide chains and the morphology of the micrometric structures formed by peptide aggregates indicates the hierarchical nature of peptide self-assembly.

In the case of **PyA5**, the hierarchy develops at the sub-nanometer scale through stacking of the Py aromatic groups and β-sheet-like alignment of the peptide chains, at the nanometer scale by ordering within small peptide fibrils, and at the micrometer scale by the intertwining of the fibrils into peptide fibers.

The globular structure of **PyA3UA** is determined at the mesoscopic scale by the predominant role of hydrophobic interaction, and, at the sub-nanometer scale by the conformational constraint of the Aib residue that inhibited the regular arrangement of Aib-substituted peptide chains in a β-sheet array, precursor of peptide fibrillation. These differences are clearly illustrated by the MD simulations, which for **PyA5** show that aromatic interactions promote the ordered stacking of the Py groups, and hence formation of structured peptide clusters that seed the directional growth of the peptide fibers.

A significant difference in the aggregation process of the two peptide analogs at the macroscale of the LB experiment is the collapse of the **PyA5** films to a solid (3D) phase, that occurs at surface

pressures definitely higher (>60 mN/m) than those observed for **PyA3UA** (<30 mN/m). This finding strongly suggests that **PyA5** is tightly packed in layered β-sheet structures, as confirmed by FTIR-ATR measurements. AFM images clearly showed that **PyA5** fibrils can tightly pack to form amyloid plaque-like clumps.

The morphological differences between the micrometric structures formed by **PyA5** and **PyA3UA**, highlighted by the AFM measurements, are undoubtedly striking and reminiscent of the analogous structures obtained driving the peptide aggregation in solution by the hydrophobic effect. More specifically, fibrillation was observed only for **PyA5**, while the Aib-substituted pentapeptide formed globular structures only.[19] However, it should be stressed that the densely-packed layers obtained for **PyA5** are a specific product of the LB methodology. Interestingly, Maltseva and Brezesinski[44] reported that the surface fibrillation rate is much faster than the rates of fibril formation observed in solution, with nucleation occurring at a much lower concentration. Our conclusion is that surface pressure can be used to modulate the morphology of self-assembling peptides and to obtain ordered arrays of densely-packed peptide fibers over extended areas.

CONCLUSION

LB experiments, fluorescence and IR absorption spectroscopy results, AFM imaging data, and MD simulations, all substantiate the same conclusion, namely that peptide aggregation is a hierarchical process, so that the morphology of the micrometric structures is dictated by the secondary structure properties of the peptide building blocks.

The results described here open two interesting perspectives. On the biomedical side, as studies on neurodegenerative diseases point to a toxic interaction between amyloid peptides and lipid membranes,[45] the evidence that a single Aib substitution can inhibit formation of peptide fibrils at the a/w interface could represent a promising approach toward the development of therapeutic peptides against the insurgence of those diseases.

On the bionanotechnology side, we showed that the LB methodology represents an excellent strategy for the preparation of peptide nano- and mesostructures coating extended areas of hydrophilic substrates. Therefore, these results may find application for the production of biocompatible platforms for biomineralization, antimicrobial coating of devices, and tissue engineering.

ASSOCIATED CONTENT

SUPPORTING INFORMATION

Fig. S1: Surface compressibility modulus K of **PyA5** (A) and **PyA3UA** (B) as a function of the mean molecular area; Fig. S2: Deconvolution of the FTIR-ATR Amide I absorption band for **PyA5** (A) and **PyA3UA** (B); Fig. S3: Angular distribution associated to the orientation of the interstrand pyrene groups. The orientation angle (θ) is the angle between two adjacent, planar pyrene moieties. Blue: **PyA5**; red: **PyA3UA**.

AUTHOR INFORMATION

Corresponding Author:

E-mail: venanzi@uniroma2.it

ORCID: 0000-0001-9364-7441

ACKNOWLEDGMENT

This project has received funding from the European Union's Horizon 2020 Research and Innovation programme under the Marie Sklodowska-Curie grant agreement No 690901. MDZ acknowledges MIUR (Futuro in Ricerca 2013, grant no. RBFR13RQXM) for support.

REFERENCES

(1) *Peptide Materials: From Nanostructures to Applications*; Aleman, C., Bianco, A., Venanzi, M., Eds.; Wiley: Chichester, U.K., 2013.

(2) Zhang, S. Fabrication of Novel Biomaterials Through Molecular Self-Assembly. *Nat. Biotech.* **2003**, *21*, 1171-1178.

(3) Adler, L.; Gazit, E. The Physical Properties of Supramolecular Peptide Assemblies: From Building Block Association to Technological Application. *Chem. Soc. Rev.* **2014**, *43*, 6881-6893.

(4) Lakshmanan, A.; Zhang, S.; Hauser, C. A. E. Short Self-Assembling Peptides as Building Blocks for Modern Nanodevices. *Trends Biotech.* **2012**, *30*, 155-165.

(5) Longo, Edoardo; Wright, Karen; Caruso, Mario; Gatto, Emanuela; Palleschi, Antonio; Scarselli, Manuela; De Crescenzi, Maurizio; Crisma, Marco; Formaggio, Fernando; Toniolo, Claudio; Venanzi, Mariano Peptide Flatlandia: A New-Concept Peptide for Positioning of Electroactive Probes in Proximity to a Metal Surface. *Nanoscale* **2015**, *7*, 15495-15506.

(6) Gatto, E.; Quatela, A.; Caruso, M.; Tagliaferro, R.; De Zotti, M.; Formaggio, F.; Toniolo, C.; Di Carlo, A.; Venanzi, M. Mimicking Nature: A Novel Peptide-based Bio-inspired Approach for Solar Energy Conversion. *ChemPhysChem* **2014**, *15*, 64-68.

(7) Semerdzhiev, S. A.; Dekker, D. R.; Subramaniam, V.; Claessens, M. A. E. Self-Assembly of Protein Fibriles into Suprafibrillar Aggregates: Bridging the Nano- and Mesoscale. *ACS Nano* **2014**, *8*, 5543-5551.

(8) Aggeli, A.; Nyrkova, I. A.; Bell, M.; Harding, R.; Carrick, L.; McLeish, T. C. B.; Semenov, A. N.; Boden, N. Hierarchical Self-Assembly of Chiral Rod-Like Molecules as a Model for β-Sheet Tapes, Ribbons, Fibrils, and Fibers. *Proc. Natl. Acad. Sci. U.S.A.* **2001**, *98*, 11857-11862.

(9) Hamley, I. W. Peptide Fibrillization. *Angew. Chem., Int. Ed.* **2007**, *46*, 8128-8147.

(10) Mandal, D.; Shirazi, A. N.; Parang, K. Self-Assembly of Peptides to Nanostructures. *Org. Biol. Chem.* **2014**, *12*, 3544-3561.

(11) Fleming, S.; Ulijn, R. Design of Nanostructures Based on Aromatic Peptide Amphiphiles. *Chem. Soc. Rev.* **2014**, *43*, 8150-8177.

(12) Gazit, E. A Possible Role for π-Stacking in the Self-Assembly of Amyloid Fibrils. *FASEB J.*, **2002**, *16*, 77-83.

(13) Toniolo, C.; Crisma, M.; Formaggio, F.; Peggion, C. Control of Peptide Conformation by the Thorpe-Ingold Effect (C^{α}-Tetrasubstitution). *Biopolymers (Pept. Sci.)* **2001**, *60*, 396-419.

(14) Venanzi, M.; Gatto, E.; Formaggio, F.; Toniolo, C. The Importance to Be Aib. Aggregation and Self-Assembly Studies on Conformationally-Constrained Oligopeptides. *J. Pept. Sci.* **2017**, *23*, 104-116.

(15) Bocchinfuso, G.; Conflitti, P.; Raniolo, S.; Caruso, M.; Mazzuca, C.; Gatto, E.; Placidi, E.; Formaggio, F.; Toniolo, C.; Venanzi, M. et al. Aggregation Propensity of Aib Homo-Peptides of Different Length: An Insight from Molecular Dynamics Simulations. *J. Pept. Sci.* **2014**, *20*, 494-507.

(16) Moretto, V.; Crisma, M.; Bonora, G.M.; Toniolo, C.; Balaram, H.; Balaram, P. Comparison of the Effect of Five Guest Residues on the β-Sheet Conformation of Host $(L\text{-Val})_n$ Oligopeptides. *Macromolecules* **1989**, *22*, 2939-2944.

(17) Formaggio, F.; Bettio, A.; Moretto, V.; Crisma, M.; Toniolo, C.; Broxterman, Q.B. Disruption of the β-Sheet Structure of a Protected Pentapeptide, Related to the β-Amyloid Sequence 17-21, Induced by a Single, Helicogenic C^{α}-Tetrasubstituted α-Amino Acid. *J. Pept. Sci.* **2003**, *9*, 461-466.

(18) Gilead, S.; Gazit, E. Inhibition of Amyloid Fibril Formation by Peptide Analogues Modified with α-Aminoisobutyric Acid. *Angew. Chem., Int. Ed.* **2004**, *43*, 4041-4004.

(19) Caruso, M.; Gatto, E.; Placidi, E.; Ballano, G.; Formaggio, F.; Toniolo, C.; Zanuy, D.; Alemàn, C.; Venanzi, M. A Single-Residue Substitution Inhibits Fibrillization of Ala-Based Pentapetides. A Spectroscopic and Molecular Dynamics Investigation. *Soft Matter* **2014**, *10*, 2508-2519.

(20) Ulman, A. *An Introduction to Ultrathin Organic Films. From Langmuir-Blodgett to Self-Assembly*; Academic Press: San Diego, CA, 1991.

(21) Kaganer, V. M.; Möhwald, H.; Dutta, P. Structure and Phase Transitions in Langmuir Monolayers. *Rev. Mod. Phys.* **1999**, *71*, 779-819.

(22) Lepère, M.; Chevallard, C.; Hernandez, J.-F.; Mitraki, A.; Guenoun, P. Multiscale Surface Self-Assembly of an Amyloid-Like Peptide. *Langmuir* **2007**, *23*, 8150-8155.

(23) Maltseva, E.; Kerth, A.; Blume, A.; Möhwald, H.; Brezesinski, G. Adsoprtion of Amyloid β-(1-40) Peptide at Phospholipid Monolayers. *ChemBioChem* **2005**, *6*, 1817-1824.

(24) Rapaport, H.; Kjaer, K.; Jensen, T.R.; Leiserowitz, L.; Tirrell, D.A. Two-Dimensional Order in β-Sheet Peptide Monolayers. *J. Am. Chem. Soc.* **2000**, *122*, 12523-12529.

(25) Rapaport, H.; Möller, G.; Knobler, C.M.; Jensen, T.R.; Kjaer, K.; Leiserowitz, L.; Tirrell, D.A. Assembly of Triple-Stranded β-Sheet Peptides at Interfaces. *J. Am. Chem. Soc.* **2002**, *124*, 9342-9343.

(26) Karjalainen, E.-L.; Barth, A. Vibrational Coupling between Helices Influences the Amide I Infrared Absorption of Proteins: Application to Bacteriorhodopsin and Rhodopsin. *J. Phys. Chem. B* **2012**, *116*, 4448-4456.

(27) Pronk, S.; Pall, S.; Schulz, R.; Larsson, P.; Bjelkman, P.; Apostolov, R.; Shirts, M.R.; Smith, J.C.; Kasson, P.M.; van der Spoel, D. *et al.* GROMACS 4.5: A High-Throughput and Highly Parallel Open Source Molecular Simulation Toolkit. *Bioinformatics* **2013**, *29*, 845-854.

(28) Oostenbrink, C.; Villa, A.; Mark, A.E.; van Gunsteren, W.F. A Biomolecular Force Field Based on the Free Enthalpy of Hydration and Solvation: The GROMOS Force-Field Parameter Sets 53A5 and 53A6. *J. Comput. Chem.* **2004**, *25*, 1656-1676.

(29) Berweger, C.D.; van Gunsteren, W.F.; Müller-Plathe, F. Force Field Parametrization by Weak Coupling. Re-engineering SPC water. *Chem. Phys. Lett.* **1995**, *232*, 429-436.

(30) Darden, T.; York, D.; Pedersen, L. Particle Mesh Ewald: An N-Log(N) Method for Ewald Sums in Large Systems. *J. Chem. Phys.* **1993**, *98*, 10089-10092.

(31) Berendsen, H.J.C.; Postma, J.P.M.; van Gunsteren, W.F.; Di Nola, A.; Haak, J.R. Molecular Dynamics with Coupling to an External Bath. *J. Chem. Phys.* **1984**, *81*, 3684-3690.

(32) Malde, A.K.; Zuo, L.; Breeze, M.; Stroet, M.; Poger, D.; Nair, P.C.; Oostenbrink, C.; Mark, A.E. An Automated Force Field Topology Builder (ATB) and Repository: Version 1.0. *J. Chem. Theory Comput.* **2011**, *7*, 4026–4037.

(33) Kato, N.; Sasaki, T.; Mukai, Y. Partially Induced Transition from Horizontal to Vertical Orientation of Helical Peptides at the Air-Water Interface and the Structure of Their Monolayers Transferred on the Solid Substrate. *Biochim. Biophys. Acta* **2015**, *1848*, 967-975.

(34) Yao, P.; Wang, H.; Chen, P.; Zhan, X.; Kuang, X.; Zhu, D.; Liu M. Hierarchical Assembly of an Achiral π-Conjugated Molecule into a Chiral Nanotube through the Air/Water Interface. *Langmuir* **2009**, *25*, 6633-6636.

(35) Chaudhary, N.; Nagaraj, R. Self-Assembly of Short Amyloidogenic Peptides at the Air-Water Interface. *J. Coll. Interf. Sci.* **2011**, *360*, 139-147.

(36) Winnik, F.M. Photophysics of Preassociated Pyrenes in Aqueous Polymer Solutions and in Other Organized Media. *Chem. Rev.* **1993**, *93*, 587-614.

(37) Bonora, G.M.; Palumbo, M.; Toniolo, C. Linear Oligopeptides. 55. Infrared Conformational Analysis of Polyethyleneglycol-Bound Alanine and Valine Homo-L-Oligopeptides in the Solid State and in Solution. *Makromol. Chem* **1979**, *180*, 1293-1304.

(38) Toniolo, C.; Palumbo, M. Solid-State Infrared Absorption Spectra and Chain Arrangement in Some Synthetic Homo-Oligopeptides in the Intermolecularly Hydrogen-Bonded Pleated-Sheet β-Conformation. *Biopolymers* **1977**, *16*, 219-224.

(39) Tatulian, S.A. in *Lipid-Protein Interactions: Methods and Protocols, Methods in Molecular Biology*; Kleinschmidt, J. H., Ed.; Springer: NewYork, 2013; Vol. 974, pp 177-218

(40) Pispisa, P.; Palleschi, A.; Stella, L.; Venanzi, M.; Mazzuca, C.; Formaggio, F.; Toniolo, C.; Broxterman, Q.B. Effects of Helical Distorsions on the Optical Properties of Amide NH Infrared Absorption in Short Peptides in Solution. *J. Phys. Chem. B* **2002**, *106*, 5733-5738.

(41) Duim, W.C.; Jiang, Y.; Shen, K.; Frydman, J.; Moerner, W.E. Super-Resolution Fluorescence of Huntingtin Reveals Growth of Globular Species into Short Fibers and coexistence of Distinct Aggregates. *ACS Chem. Biol.* **2014**, *9*, 2767-2778.

(42) Lepère, M.; Chevallard, C.; Brezesinski, G.; Goldmann, M.; Guenoun, P. Crystalline Amyloid Structures at Interfaces. *Angew. Chem. Int. Ed.* **2009**, *48*, 5005-5009.

(43) Ferrão_Gonzales, A.D.; Souto, S.O.; Silva, J.L.; Foguel, D. The Preaggregated State of an Amyloidogenic Protein: Hydrostatic Pressure Converts Native Transthyretin into the Amyloidogenic State. *Proc. Natl. Acad. Sci. U.S.A.* **2000**, *97*, 6445-6450.

(44) Maltseva, E.; Brezesinski, G. Adsorption of Amyloid Beta (1-40) Peptide to Phosphatidylethanolamine Monolayers. *ChemPhysChem* **2004**, *5*, 1185-1190.

(45) Bokvist, M.; Lindström, F.; Watts, A.; Gröbner, G. Two Types of Alzheimer's B-Amyloid (1-40) Peptide Membrane Interactions: Aggregation Preventing Transmembrane Anchoring Versus Accelerated Surface Fibril Formation. *J. Mol. Biol.* **2004**, *335*, 1039-1049.

Table of Content Graphic